The University of
Nottingham

UNITED KINGDOM · CHINA · MALAYSIA

Chen, Sheng and Yang, Bo and Zheng, Chuguang (2016) A lattice Boltzmann model for heat transfer in heterogeneous media. International Journal of Heat and Mass Transfer, 102 . pp. 637-644. ISSN 0017-9310

Access from the University of Nottingham repository:
http://eprints.nottingham.ac.uk/34698/1/LBforvariedproperties.pdf

A lattice Boltzmann model for heat transfer

in heterogeneous media

Sheng Chen [*1,2,3] Bo Yang [1] Chuguang Zheng [1]

1. State Key Laboratory of Coal Combustion, Huazhong University of Science and Technology, Wuhan 430074, China

2. Institute for Modelling and Simulation in Fluodynamics, Nanoscience and Industrial Mathematics "Gregorio Millán Barbany", Universidad Carlos III de Madrid, Leganes 28911, Spain

3. Faculty of Engineering, The University of Nottingham, University Park, Nottingham NG7 2RD, UK

* Corresponding author. Faculty of Engineering, University of Nottingham. E-mail address: shengchen.hust@gmail.com

Abstract

So far the lattice Boltzmann (LB) method has matured as a powerful tool to address a diversity of heat and mass transfer challenges. For most practical applications, the variation of thermophysical properties of working media will influence the performance of industrial systems substantially. However, nowadays the efforts to improve the LB method to consider variable thermophysical properties of working media are quite sparse. In the present work we firstly analyze the shortcomings of the available

LB approaches for modeling working fluid with variable thermophysical properties. Based on the analysis, a simple LB model is proposed to overcome these shortcomings. The feasibility and reliability of the new LB model have been validated by three simple but nontrivial benchmark tests. Although it is originally proposed to simulate fluid flow with variable thermophysical properties, the present model can be extended directly to some other research areas where variation of thermophysical properties of working media should be considered, such as conjugate heat transfer between solid materials.

Key words: Lattice Boltzmann method; heat and mass transfer; variable thermophysical properties; heterogeneous media

1 Introduction

With the rapid development of computer science, numerical simulation has become a powerful, sometimes even a unique, tool to address a diversity of challenges in various practical applications. In the fields relevant to heat and mass transfer in fluid flow, computational fluid dynamics (CFD) techniques have been popularly adopted as a cost-effective way for system design, diagnosis and optimization. Due to the extreme complication of fluid flow in engineering, during the past decades various modeling approaches and numerical solvers have been continuously proposed to conquer the difficulties and to present a clearer physical picture of the investigated problems [1]. Among them, the lattice Boltzmann (LB) method has attracted significant attention owing to its

some intrinsic advantages, such as modeling interaction, in a mesoscopic level, between different phases/components in multiphase/multicomponent flow and a thermodynamics-consistent description of turbulence [2]. Until now, LB-based approaches have been widely used not only to deepen our insight into numerous fundamental research areas [3–5], but also to constitute commercial software to optimize industrial processes [6]. On the topics relevant to heat transfer, the LB method has reached a great achievement over a wide range, such as enhanced heat transfer by nanofluid [7–10], micro-scale heat transfer [11–13] and conjugate heat transfer[14,15].

The LB method is a type of mesoscopic approach which implies it will not solve macroscopic governing equations directly as conventional CFD tools do, although macroscopic phenomena can be reproduced by it satisfactorily. All available LB-based approaches start from the so-called LB equation which can be regarded as a special discretization of the Boltzmann equation [2]. Through a multiscale expansion, some well-known macroscopic governing equations, such as the Euler and/or Navier-Stokes equation, can be recovered from the LB equation with different truncated errors [4]. Accordingly, in the recovered macroscopic governing equations all parameters representing the thermophysical properties of working media (e.g. specific heat capacity, thermal conductivity and dynamic viscosity) are determined through the multiscale expansion. In order to exactly match the macroscopic governing equations in CFD, a number of macroscopic quantities in the recovered macroscopic e-

quations, including thermophysical properties of working media, are assumed to be constant or to vary slightly across the investigated domain. Original-ly, the LB method was developed as an alternative solver for isothermal low Mach number flow simulation, so such assumption was tenable. Later, the LB method was extended to model thermal flow and reaction flow[5]. Surprisingly, although the thermophysical properties of working media may be significantly different temporally and/or spatially in those scenarios, the above assumption has still been adopted implicitly. In spite of acceptable simulation results hav-ing been reproduced in some scenarios, it is not physical sound. Especially, in theory the applicable scope of these LB approaches has been limited not to exceed the relaxation of the above assumption too much, which can not meet the requirements of most practical applications.

Nowadays, the available open literature, attempting to model temporally/spatially different thermophysical properties of working media by the LB method, is quite sparse. Guo and Zhao [16] perhaps are the pioneers to consider how to model changeable dynamic viscosity of working fluid in the framework of the LB method. In Ref.[16], natural convection of a fluid with temperature-dependent viscosity was simulated. The influence of variable viscosity on heat transfer has been presented by the authors and it was observed the standard LB model's prediction, in which constant viscosity assumption adopted, would significantly deviate the real phenomena. However, there are still two implic-it assumptions in Guo's LB model: (1) the density change of working fluid

4

should be very small and (2) the specific heat capacity and thermal conductivity of working fluid should be constant. Unfortunately, in many industrial applications (e.g. combustion), these two assumptions can hardly be met. Recently, some scholars discussed how to model conjugate heat transfer by the LB method [17–22]. For conjugate heat transfer, the investigated domain is consisted of several different medium layers, and the specific heat capacity and/or thermal conductivity of the medium layers may be different with each other. However, their LB approaches can not treat spatially consecutive variation of thermophysical properties within any medium layer as in their models the thermophysical properties of each medium layer must to be spatially identical. On the other words, these LB models for conjugate heat transfer aim to handle interfaces between heterogeneous medium layers rather than to model variable thermophysical properties of working media.

This drawback has hampered the maturation of the LB method as an industrial-level CFD tool. In order to bridge this gap, in this work we try to establish a LB model which can deal with variable thermophysical properties of working media simply and efficiently. As shown by the above literature survey, this issue has been ignored by the LB community although it is extremely critical for practical applications. What should be emphasized is although in the present study we only take a single-relaxation-time LB model as an example to show how to address the variation of thermophysical properties of working media, the extension to its multiple-relaxation-time counterpart is straightforward

[5,18].

2 LB model considering variation of thermophysical properties

The standard macroscopic governing equations for industrial fluid flow with variable thermophysical properties, in their tensor formulation, read [1]:

$$\partial_t \rho + \nabla_\alpha \rho u_\alpha = 0, \tag{1}$$

$$\partial_t \rho u_\alpha + \nabla_\beta \rho u_\alpha u_\beta = -\nabla_\alpha p + \nabla_\beta \mu (\nabla_\alpha u_\beta + \nabla_\beta u_\alpha), \tag{2}$$

$$\partial_t \rho C_p T + \nabla_\alpha \rho C_p T u_\alpha = \nabla_\alpha \lambda \nabla_\alpha T. \tag{3}$$

where ρ, u_α, p and T are the density, velocity, pressure and temperature of working fluid. In addition, μ, λ and C_p are the thermophysical properties of working fluid and they denotes the dynamic viscosity, thermal conductivity and constant pressure specific heat capacity, respectively.

However, the recovered macroscopic governing equations by the standard LB method read[2,4]:

$$\partial_t \rho + \nabla_\alpha \rho u_\alpha = 0, \tag{4}$$

$$\partial_t \rho u_\alpha + \nabla_\beta \rho u_\alpha u_\beta = -\nabla_\alpha p + \nabla_\beta \nu (\nabla_\alpha \rho u_\beta + \nabla_\beta \rho u_\alpha), \tag{5}$$

$$\partial_t \rho C_p T + \nabla_\alpha \rho C_p T u_\alpha = \nabla_\alpha \kappa \nabla_\alpha \rho C_p T. \tag{6}$$

where $\nu = \mu/\rho$ and $\kappa = \lambda/(\rho C_p)$ are the kinematic viscosity and thermal

6

diffusivity of working fluid, respectively. One can observe there are obvious differences between the recovered macroscopic governing equations Eqs.(5)-(6) and the standard macroscopic governing equations Eqs.(2)-(3): firstly, the second term on the right side of Eq.(5) does not match that in Eq.(2) exactly; secondly, the last term of Eq.(6) is not the same as that in Eq.(3).

The second term on the right side of Eq.(5) $\nabla_\beta \nu (\nabla_\alpha \rho u_\beta + \nabla_\beta \rho u_\alpha)$ can be transformed as

$$\nabla_\beta \nu (\nabla_\alpha \rho u_\beta + \nabla_\beta \rho u_\alpha) = \nabla_\beta \mu (\nabla_\alpha u_\beta + \nabla_\beta u_\alpha) + \nabla_\beta \nu (u_\beta \nabla_\alpha \rho + u_\alpha \nabla_\beta \rho). \quad (7)$$

Therefore, Eq.(5) can approximate to Eq.(2) only when the spatial derivation of density is slight. For example, for isothermal low Mach number flow, there is $O(\nabla_\alpha \rho) \sim O(Ma^2)$ [23], so the equality Eq.(7) can be written as

$$\nabla_\beta \nu (\nabla_\alpha \rho u_\beta + \nabla_\beta \rho u_\alpha) = \nabla_\beta \mu (\nabla_\alpha u_\beta + \nabla_\beta u_\alpha) + O(Ma^2). \quad (8)$$

where Ma is the Mach number. What should be emphasized is that the equality Eq.(8) may collapse in some low Mach number scenarios, such as in low Mach number combustion where the spatial derivation of density is large [24]. In the LB community, there is a commonly found mistake that many scholars take the low Mach number flow equivalent to $O(\nabla_\alpha \rho) \sim O(Ma^2)$. Strictly, such equivalence can stand only in isothermal low Mach number flow.

The last term in Eq.(6) can be rewritten as

$$\nabla_\alpha \kappa \nabla_\alpha \rho C_p T = \nabla_\alpha \lambda \nabla_\alpha T + \nabla_\alpha \kappa T \nabla_\alpha \rho C_p. \qquad (9)$$

Accordingly, Eq.(6) can match Eq.(3) exactly only when $\nabla_\alpha \rho C_p = 0$ which implies at least C_p should be a constant across the investigated domain. As discussed below, it is the reason why it is difficult to adopt the standard LB approach to treat conjugate heat transfer.

In order to recover the macroscopic governing equations Eqs.(1)-(3) exactly without the above restrictions, in the present study a double-distribution-function LB model is proposed. The present model is partially based on our previous LB model developed for low Mach number combustion simulation[24], in which the flow and scale (e.g. temperature) fields are solved by two sets of distribution functions, respectively.

2.1   Flow field

The evolving equation for the flow field reads

$$f_k(x_\alpha + ce_{\alpha k}\Delta t, t + \Delta t) - f_k(x_\alpha, t) = -\tau_u^{-1}[f_k(x_\alpha, t) - f_k^{(eq)}(x_\alpha, t)]. \qquad (10)$$

where $f_k(x_\alpha, t)$ is the distribution function at space x_α and time t with velocity $ce_{\alpha k}$ and $f_k^{(eq)}(\mathbf{x}, t)$ is the corresponding equilibrium distribution. $e_{\alpha k}$ is the

8

discrete velocity direction, which depends on the lattice model adopted and $k = 0$ represents the stationary fluid particle. Δx, Δt and τ_u are the lattice grid spacing, evolving time step and dimensionless relaxation time for the flow field, respectively. $c = \Delta x / \Delta t$ is the pseudo-fluid particle speed.

The equilibrium distribution in the present model is defined by

$$f_k^{(eq)} = \chi_k p + \rho s_k(u_\alpha), \tag{11}$$

where

$$s_k(u_\alpha) = \zeta_k \left[\frac{c e_{k\alpha} u_\alpha}{c_s^2} + \frac{(c e_{k\alpha} u_\alpha)(c e_{k\beta} u_\beta)}{2 c_s^4} - \frac{u_\alpha u_\alpha}{2 c_s^2} \right].$$

In the above equation ζ_k represents the weight coefficients which are the same as those in the standard LB method [2,4], and the parameter c_s satisfies $c_s^2 \delta_{\alpha\beta} = \sum_k \zeta_k c^2 e_{k\alpha} e_{k\beta}$ [24]. The parameter χ_k is given by [24]

$$\chi_k|_{k \neq 0} = \zeta_k / c_s^2, \chi_0 = \frac{\rho}{\rho} + \frac{\zeta_0 - 1}{c_s^2}. \tag{12}$$

The pressure, momentum and dynamic viscosity of working fluid can be obtained by [24]

$$p = \frac{c_s^2}{1 - \zeta_0} \left[\sum_{k \neq 0} f_k + \rho s_0(u_\alpha) \right], \tag{13}$$

$$\rho u_\alpha = \sum_k c e_{k\alpha} f_k, \tag{14}$$

9

$$\mu(T) = \rho(\tau_u - 1/2)c_s^2\Delta t. \tag{15}$$

With the aid of the state equation $p = c_s^2\rho$, the density and velocity of flow field can be calculated out.

The symbol $\mu(T)$ in Eq.(15) denotes the dynamic viscosity is changeable and here it is a function of temperature of working media as in most practical applications the dynamic viscosity of working fluid is only highly temperature-dependent [1]. However, it is not difficult to extend the present model to consider other influences on variation of the dynamic viscosity (e.g. composition fluctuation in multicomponent flow) [24]. Furthermore, as pointed out in Ref.[24], the relaxation time τ_u in Eq.(10) is a field variable which depends on local temperature in the present work. Make an comparison between Eqs.(10)-(11) in the present work and Eqs.(11)-(12) in Ref.[24], one can find that for flow field simulation, the present approach is nearly the same as that in Ref.[24] because Eqs.(1)-(2) can be recovered exactly from Eqs.(11)-(12) in Ref.[24], without the assumption that spatial derivation of density should be a slight quantity. In the present work the step of rescaling pseudo-fluid particle speed that proposed in Ref.[24] is not included as such rescaling step is only required for combustion simulation. In addition, if in the investigated domain $O(\nabla_\alpha\rho) \sim O(Ma^2)$ always can be met, a standard LB model can also be used for flow field simulation, as demonstrated in Ref.[24], Eqs.(10)-(11) will reduce to an incompressible LB model for fluid flow simulation.

In the following section the evolving equation for temperature field will be discussed. In fact, the major difference between the present model and the LB approach designed in Ref.[24] is reflected by temperature field modeling as in Ref.[24] C_p and λ both were assumed constant.

2.2 Temperature field

In order to treat the variation of C_p and λ across the investigated domain, a new evolving equation for temperature field is proposed in the present study, which reads

$$g_j(x_\alpha + ce_{\alpha,j}\Delta t, t + \Delta t) - g_j(x_\alpha, t) = -\tau_T^{-1}[g_j(x_\alpha, t) - g_j^{(eq)}(x_\alpha, t)]. \quad (16)$$

In Eq.(16) τ_T is the dimensionless relaxation time for temperature field simulation.

The equilibrium distribution in Eq.(16) reads

$$g_j^{(eq)} = \begin{cases} \rho T(C_p - C_{p0}) + \omega_j C_p T(\frac{\rho_0 C_{p0}}{C_p} + \frac{\rho c e_{j\alpha} u_\alpha}{c_s^2}), & j = 0 \\[2ex] \omega_j C_p T(\frac{\rho_0 C_{p0}}{C_p} + \frac{\rho c e_{j\alpha} u_\alpha}{c_s^2}), & j \neq 0 \end{cases} \quad (17)$$

where ω_j represents the weight coefficients and e_j denotes the discrete velocity direction. ρ_0 and C_{p0} are the density and constant pressure specific heat capacity at the reference temperature T_0. The parameter c_s satisfies

$c_s^2 \delta_{\alpha\beta} = \sum\limits_{j} \omega_j c^2 e_{j\alpha} e_{j\beta}$. One can observe the lattice used for solving temperature field is different from that for velocity field as Eq.(3) is an advection-diffusion equation for which a simpler lattice is sufficient [2,4]. For example, a D2Q5 lattice for two-dimensional problems and a D3Q7 lattice for three-dimensional domains [18,24]. Such choice can save computational cost efficiently, which is crucial for industrial-level simulation, as explained in our previous work [24].

If one would like to use the same lattice for flow field simulation to solve temperature field, the equilibrium distribution in Eq.(16) will read

$$
g_j^{(eq)} = \begin{cases} \rho T(C_p - C_{p0}) + \zeta_j C_p T\{\frac{\rho_0 C_{p0}}{C_p} + \rho[\frac{ce_{j\alpha}u_\alpha}{c_s^2} + \frac{(ce_{k\alpha}u_\alpha)(ce_{k\beta}u_\beta)}{2c_s^4} - \frac{u_\alpha u_\alpha}{2c_s^2}]\}, & j = 0 \\[4mm] \zeta_j C_p T\{\frac{\rho_0 C_{p0}}{C_p} + \rho[\frac{ce_{j\alpha}u_\alpha}{c_s^2} + \frac{(ce_{k\alpha}u_\alpha)(ce_{k\beta}u_\beta)}{2c_s^4} - \frac{u_\alpha u_\alpha}{2c_s^2}]\}, & j \neq 0 \end{cases}
$$
(18)

The temperature T is obtained by

$$
T = \frac{\sum\limits_{j} g_j}{\rho C_p}.
$$
(19)

and the thermal conductivity λ is given by

$$
\lambda = (\tau_T - 1/2)c_s^2 \Delta t \rho_0 C_{p0}.
$$
(20)

where τ_T must be a field variable as λ may vary across the investigated domain.

12

The detailed process to recover Eqs.(1)-(2) from the evolving equations Eqs.(10)-(11) has been presented in Ref.[24], so it is not repeated here for simplicity. In this section we focus on how to recover Eq. (3) through multiscale expansion of Eqs. (16)-(17).

Equation (16) can be expanded in Taylor series as [2]

$$\Delta t(\partial_t + ce_{j\alpha}\nabla_\alpha)g_j + \frac{\Delta t^2}{2}(\partial_t + ce_{j\alpha}\nabla_\alpha)^2 g_j + \frac{1}{\tau_T}[g_j - g_j^{eq}] = O(\Delta t^3). \quad (21)$$

Introducing the multiscale expansion $\partial_t = \epsilon\partial_{t1} + \epsilon^2\partial_{t2}$, $\nabla_\alpha = \epsilon\nabla_{\alpha1}$ and $g_j = g_j^{(eq)} + \epsilon g_j^{(1)} + \epsilon^2 g_j^{(2)} + O(\epsilon^3)$ [4], we can sort Eq. (21) in terms of ϵ and ϵ^2 as

$$(\partial_{t1} + ce_{j\alpha}\nabla_{\alpha1})g_j^{(eq)} = -\frac{g_j^{(1)}}{\Delta t\tau_T} + O(\epsilon). \quad (22)$$

$$\partial_{t2}g_j^{(eq)} + (\partial_{t1} + ce_{j\alpha}\nabla_{\alpha1})[(1 - \frac{1}{2\tau_T})g_j^{(1)}] = -\frac{g_j^{(2)}}{\Delta t\tau_T} + O(\epsilon^2). \quad (23)$$

As mentioned above, for temperature field modeling there are two choices on lattice model, here we adopt a simpler one whose equilibrium distribution is described by Eq.(17) (the process is similar if Eq.(18) adopted). With the symmetry properties of the lattice $\sum_j \omega_j ce_{j\alpha} = 0$ and $\sum_j \omega_j ce_{j\alpha}ce_{j\beta} = c_s^2\delta_{\alpha\beta}$ we can obtain

$$\sum_j g^{(eq)} = \rho C_p T, \quad (24)$$

$$\sum_j ce_{j\alpha}g^{(eq)} = \rho C_p T u_\alpha, \tag{25}$$

$$\sum_j ce_{j\alpha}ce_{j\beta}g^{(eq)} = \rho_0 C_{p0} T c_s^2 \delta_{\alpha\beta}. \tag{26}$$

Please bear in mind that the second moment of $g^{(eq)}$ (namely Eq.(26)) is different from that of the standard LB method. We will discuss it below.

With the aid of Eqs.(24)-(26), as well as $\sum_j g_j^{(1)} = \sum_j g_j^{(2)} = 0$, the summation of Eqs.(22)-(23) over the discrete direction $e_{j\alpha}$ reads

$$\partial_{t1}\rho C_p T + \nabla_{\alpha 1}\rho C_p T u_\alpha = 0 + O(\epsilon), \tag{27}$$

$$\partial_{t2}\rho C_p T + \nabla_{\alpha 1}[c_s^2(\frac{1}{2} - \tau_T)\Delta t \nabla_{\alpha 1}\rho_0 C_{p0}T] = 0 + O(\epsilon^2). \tag{28}$$

Because ρ_0 and C_{p0} are constant across the whole investigated domain, $\nabla_{\alpha 1}\rho_0 C_{p0}T = \rho_0 C_{p0}\nabla_{\alpha 1}T$. Accordingly Eq.(28) can be re-written as

$$\partial_{t2}\rho C_p T + \nabla_{\alpha 1}[c_s^2(\frac{1}{2} - \tau_T)\Delta t \rho_0 C_{p0}\nabla_{\alpha 1}T] = 0 + O(\epsilon^2). \tag{29}$$

Combining Eqs.(27) and (29), we can obtain the final recovered macroscopic governing equation for temperature field

$$\partial_t \rho C_p T + \nabla_\alpha \rho C_p T u_\alpha = \nabla_\alpha \lambda \nabla_\alpha T + O(\epsilon^2). \tag{30}$$

where $\lambda = c_s^2(\tau_T - \frac{1}{2})\Delta t \rho_0 C_{p0}$. It is obvious that Eq.(30) can match Eq.(3) exactly, no matter how λ and/or C_p vary spatially.

14

The advantage of the present model benefits from Eq.(26). In all available LB models, the second moment of the equilibrium distribution always generates $\sum_{j} ce_{j\alpha} ce_{j\beta} g^{(eq)} = \rho C_p T c_s^2 \delta_{\alpha\beta} + O(\epsilon^2)$, so the recovered macroscopic equation reads

$$\partial_t \rho C_p T + \nabla_\alpha \rho C_p T u_\alpha = \nabla_\alpha [c_s^2 (\tau_T - \frac{1}{2}) \Delta t \nabla_\alpha \rho C_p T] + O(\epsilon^2). \qquad (31)$$

which implies if $\nabla_\alpha \rho C_p \neq 0$, namely ρ and/or C_p varying spatially across the investigated domain, the quantity that really evolves in the previous L-B models is $\rho C_p T$ rather than T. Therefore, for conjugate heat transfer, in the framework of the standard LB framework, across the interface between heterogeneous working media only the continuity of $\rho C_p T$ can be guaranteed, rather than that of T.

Although originally it is design to treat variation of thermophysical properties of working fluid, the present model can be used to model heat transfer in solid material with variable thermophysical properties, by turning off Eq.(10) and setting $u_\alpha = 0$ in the equilibrium distribution Eq.(32). Moreover, the present model can be directly used for conjugate heat transfer simulation, without any modification. Compared with some of the available LB approaches for conjugate heat transfer simulation [17–20], the present model is easier to be implemented as here no interface should be treated explicitly. Although the complexity induced by interface treatment can be avoided in several previous

15

LB models [21,22], they suffer a number of obvious shortcomings. In Ref.[21], to meet the conjugate heat transfer condition, a source term was designed and added to the LB evolving equation. However, the source term is a non-local operator with only first-order accuracy. In addition, how to determine the source term will become a great challenge if the interface is not located at the half-way between two lattice grids. At first glance, the present model looks a little similar with that proposed by Huang et al.[22], but in their model the density of each component of working media should be identical. Such limitation restricts the applicable range of Huang's model as in practical applications the density of different working media usually is not the same. More important, except crossing the interface, thermophysical properties of working media can not vary spatially/temporally in almost all of the afore-mentioned models. These disadvantages have been remedied by the present model through a straightforward way and it will be demonstrated in the next section. If the step of re-scaling pseudo-fluid particle speed that proposed in Ref.[24] is included, the present model can be extended straightforwardly for low Mach number combustion simulation where ρ, μ, C_p and λ all may vary significantly in the vicinity of flames.

3 Numerical validation

In order to validate the present model, three simple but non-trivial benchmark tests are adopted. The D2Q9 lattice is used for solving flow field and the D2Q5 lattice is employed to compute temperature field, similar with our previous work [24].

3.1 Planar thermal Poiseuille flow with two immiscible fluids

Figure 1 illustrates the schematic configuration of the planar thermal Poiseuille flow with two immiscible fluids. The temperature on top wall of the channel is T_2 and that on the bottom wall is T_1. Here we set $T_2/T_1 = 2$. These two fluids have the same density and dynamic viscosity, namely $\rho_1 = \rho_2$ and $\mu_1 = \mu_2$. It is assumed the flow can keep straight stably, so a stable horizontal interface ,represented by the red dashed line in Fig. 2, between the immiscible fluids can be formed. However, their pressure specific heat capacity and thermal conductivity may be different.

Firstly, we set $C_{p1} = C_{p2}$ and $\lambda_1 = \lambda_2$, so it is equivalent to single-phase planar thermal Poiseuille flow and an analytic solution is available [25]. Figure 2 plots the numerical data obtain by the present model, compared with the analytic results. The numerical prediction agrees well with the analytic data.

Then we set $C_{p2} = 3C_{p1}$ and $\lambda_2 = 10\lambda_1$. Figure 3 shows the numerical results

obtain by the present model, compared with that by the finite volume method (FVM) [1]. There is a good agreement between them.

3.2 Conjugate heat transfer between solid media

If the motional working fluids in Fig.1 are replaced by two different types of stationary solid material, then it becomes another benchmark test, namely conjugate heat transfer between solid media, as discussed in Ref.[17]. In Ref.[17], $\rho_2 C_{p2} = 1.5 \rho_1 C_{p1}$ and $\lambda_2 = 3\lambda_1$. The corresponding analytic solution of temperature profile reads [17]

$$
T(y) = \begin{cases}
\frac{3y}{2H}(T_2 - T_1) + T_1, & 0 \le y \le 0.5H. \\
\\
(\frac{y}{2H} + 0.5)(T_2 - T_1) + T_1, & 0.5H \le y \le H.
\end{cases}
$$

For the LB model designed in Ref.[22], the density of each component of working media should be identical. The present model is not subject to such limitation and can work well when $\rho_1 \neq \rho_2$.

Figure 4 illustrates the numerical data obtain by the present model, compared with the analytic results. There is no obvious difference between them. The continuity of temperature and of temperature gradient across the interface of solid media can be guaranteed exactly in the present numerical prediction, which is important for conjugate heat transfer simulation[17–21]. Furthermore,

18

in the models proposed in Refs.[17–21], the thermophysical properties of each
solid material layer should be assumed spatially identical, but such assumption
may not meet the requirements of real situations. In the present model, such
restriction does not exist and the thermophysical properties of each solid ma-
terial layer can vary arbitrarily. Taking the above benchmark as an example,
here we assume C_p and λ of each solid layer both are temperature-dependent
and their relationships read

$$Cp_1(T) = -5.56(T - T_1) + Cp_1(T_1), \lambda_1(T) = T\lambda_1(T_1)/T_1.$$

$$Cp_2(T) = 15.79(T - T_1) + Cp_2(T_1), \lambda_2(T) = T\lambda_2(T_1)/T_1.$$

where $Cp_2(T_1) = 1.5Cp_1(T_1)$ and $\lambda_2(T_1) = 3\lambda_1(T_1)$. Namely, the initial and
boundary conditions are the same as those in the above case but now C_p
and λ of each solid layer will change across the domain. Figure 5 depicts
the temperature profile, compared with its counterpart assuming constant
thermophysical properties. It can be observed there is an obvious difference
caused by variable thermophysical properties of solid materials.

3.3   Forced convection in lid-driven square cavity

The configuration of lid-driven forced convection in a square cavity is shown
by Fig.6, where $T_0 = 1.0$ and $u_0 = 1.0$.

19

Firstly, we assume the thermophysical properties of working fluid are constant. Figure 7 illustrates the profiles of temperature and velocity obtained by the present method, compared with those presented in our previous publication by a vorticity-streamfunction approach [26]. The Reynolds number is defined as $Re = \rho_0 u_0 H / \mu_0$, where μ_0 is the dynamic viscosity of working fluid at T_0. The present prediction agrees well with that by the vorticity-streamfunction approach proposed in Ref.[26].

In succession, we consider the influence of variable thermophysical properties of working fluid on flow and heat transfer. We assume μ, Cp and λ all are temperature-dependent, and

$$\mu(T) = 0.5 T \mu_0 / T_0,$$

$$Cp(T) = 0.5632(T - T_0) + Cp_0,$$

$$\lambda(T) = T \lambda_0 / T_0.$$

In the present work we set $Cp_0 = 2.5$.

Figure 8 plots the streamlines and isotherm lines. One can observe the flow field and temperature field with variable thermophysical properties are obviously different from their counterparts with constant thermophysical properties. Compared with its counterpart with constant thermophysical properties, the vortex at the bottom-right corner of the square cavity will be compressed due to variable thermophysical properties. Meanwhile, a secondary small vor-

tex will emerge at the bottom-left corner, which is not obvious in its counterpart with constant thermophysical properties. In addition, the isothermal lines in the vicinity of the left and bottom walls are much denser in the case with variable thermophysical properties, which implies more intensive heat transfer. The observation can be supported by Table 1, where the subscript l, r, t and b denote the left, right, top and bottom wall, respectively. Due to the variation of thermophysical properties, heat exchange on the left, top and bottom wall will be enhanced significantly, especially Nu_l and Nu_b are almost three times as large as their counterpart in constant thermophysical property situation. However, on the right wall heat exchange will be suppressed seriously. Such changes are crucial for heat exchanger design in industries.

Figure 9 illustrates the profiles of temperature and velocity along the centerlines of the cavity. Through this figure, the influence of variation of thermophysical properties on flow and temperature field can be observed more clearly, especially through the comparison between the temperature profiles.

4 Conclusion

For most practical applications, the variation of thermophysical properties of working media will critically influence the performance of industrial systems. Until now the LB method has matured as a powerful tool to address a diversity of challenges in industries, besides in basic research. However, so far the efforts

21

to improve the LB method considering variable thermophysical properties of working media are still few. This drawback has hampered the LB method to become an industrial-level accepted numerical tool. In the present work we firstly analyze the shortcomings of the available LB approaches when they are used to simulate heat and mass transfer of working media with changeable thermophysical properties. In succession, based on the analysis, a simple LB model is proposed to overcome these shortcomings. The feasibility and reliability of the new LB model has been validated by three simple but nontrivial benchmark tests. The numerical results demonstrate the present model can capture the influences of variable thermophysical properties of working media exactly and effectively. Especially, the present model can be extended directly to investigate some other topics where variation of thermophysical properties of working media should be considered, such as conjugate heat transfer. Compared with the available LB models for conjugate heat transfer simulation, the present model is more efficient as complicated interface treatment is avoided.

The present model can also be used to simulate heat and mass transfer restricted by complicated domains if the available curved boundary treatment schemes [5] are incorporated. Furthermore, the present model can be adopted straightforwardly to simulate low Mach number combustion [24] as in combustion thermophysical properties of reactants will change substantially.

Finally, although in the present study we only take a single-relaxation-time LB model as an example to show how to address the variation of thermophys-

ical properties of working media, the extension to its multiple-relaxation-time counterpart is straightforward [5,18]. It will be considered in our future work.

Acknowledgments

References

[1] Chung T.J. Computational Fluid Dynamics. Cambridge:Cambridge University Press; 2002.

[2] Succi S. The lattice Boltzmann equation for fluid dynamics and beyond. Oxford: Oxford university press;2001.

[3] Benzi R, Succi S, Vergassola M. The lattice Boltzmann equation: theory and applications. Physics Reports 1992;222:145-197.

[4] Chen S, Doolen GD. Lattice Boltzmann Method for Fluid Flows. Annual Review

of Fluid Mechanics 1998;30:329-364.

[5] Aidun CK, Clausen JR. Lattice-Boltzmann Method for Complex Flows. Annual Review of Fluid Mechanics 2010;42: 439-472.

[6] Chen H, Kandasamy S, Orszag S, Shock R, Succi S, Yakhot V. Extended Boltzmann Kinetic Equation for Turbulent Flows. Science 2003;301:633-636.

[7] Chen S, Yang B, Luo KH, Xiong X, Zheng C. Double diffusion natural convection in a square cavity filled with nanofluid. International Journal of Heat and Mass Transfer 2016;95: 1070-1083

[8] Sheikholeslami M, Ellahi R. Three dimensional mesoscopic simulation of magnetic field effect on natural convection of nanofluid. International Journal of Heat and Mass Transfer 2015;89:799-808

[9] Sheikholeslami M, Ellahi R, Hassan M, Soleimani S. A study of natural convection heat transfer in a nanofluid filled enclosure with elliptic inner cylinder. International Journal of Numerical Methods for Heat Fluid Flow 2014;24:1906-1927

[10] Kefayati GHR. FDLBM simulation of mixed convection in a lid-driven cavity filled with non-Newtonian nanofluid in the presence of magnetic field. International Journal of Thermal Sciences 2015;95:29-46

[11] Li L, Zhou L, Yang M. An Expanded Lattice Boltzmann Method for Dual Phase Lag model. International Journal of Heat and Mass Transfer 2016;93:834-838

[12] Gokaltun S, Dulikravich GS. Lattice Boltzmann method for rarefied channel flows with heat transfer. International Journal of Heat and Mass Transfer

2014;78:796-804

[13] Mao Y, Xu M. Lattice Boltzmann numerical analysis of heat transfer in nano-scale silicon films induced by ultra-fast laser heating. International Journal of Thermal Sciences 2015;89:210-221

[14] Seddiq M, Maerefat M, Mirzaei M. Modeling of heat transfer at the fluidCsolid interface by lattice Boltzmann method. International Journal of Thermal Sciences 2014;75: 28-35

[15] Taghilou M, Rahimian MH. Lattice Boltzmann model for thermal behavior of a droplet on the solid surface. International Journal of Thermal Sciences 2014;86:1-11

[16] Guo ZL, Zhao TS. Lattice Boltzmann simulation of natural convection with temperature-dependent viscosity in a porous cavity. Progress in Computational Fluid Dynamics 2005;5: 110-117

[17] Hu Y, Li D, Shu S, Niu X. Full Eulerian lattice Boltzmann model for conjugate heat transfer. Physical Review E 2015;92:063305/1-063305/12

[18] Le G, Oulaid O, Zhang JF. Counter-extrapolation method for conjugate interfaces in computational heat and mass transfer. Physical Review E 2015;91:033306/1-033306/11

[19] Li L, Chen C, Mei R, Klausner JF. Conjugate heat and mass transfer in the lattice Boltzmann equation method. Physical Review E 2014;89:043308/1-043308/21.

[20] Guo K, Li L, Xiao G, Yeung AN, Mei R. Lattice Boltzmann method for

conjugate heat and mass transfer with interfacial jump conditions. International Journal of Heat and Mass Transfer 2015;88: 306-322

[21] Karani H, Huber C. Lattice Boltzmann formulation for conjugate heat transfer in heterogeneous media. Physical Review E 2015;91:023304/1-023304/10.

[22] Huang R, Wu H. Phase interface effects in the total enthalpy-based lattice Boltzmann model for solid-liquid phase change. Journal of Computational Physics 2015;294:346-362

[23] He XY, Luo LS. Lattice Boltzmann model for the incompressible Navier-Stokes equation. Journal of Statistical Physics 1997;88:927-944.

[24] Chen S, Liu Z, Zhang C, He Z, Tian Z, Shi B, Zheng C. A novel coupled lattice Boltzmann model for low Mach number combustion simulation. Applied Mathematics and Computation 2007;193 : 266-284.

[25] Chen S, Luo K, Zheng C. A simple enthalpy-based lattice Boltzmann scheme for complicated thermal systems. Journal of Computational Physics 2012;231:8278-8294.

[26] Chen S, Tolke J, Krafczyk M. A new method for the numerical solution of vorticity-streamfunction formulations. Computer Methods in Applied Mechanics and Engineering 2008;198:367-376
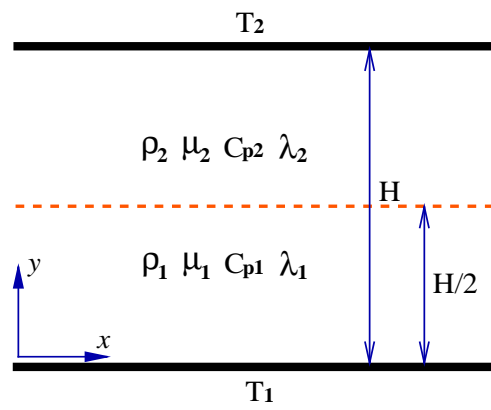
Fig. 1. Schematic configuration of planar thermal Poiseuille flow with horizontal interface.
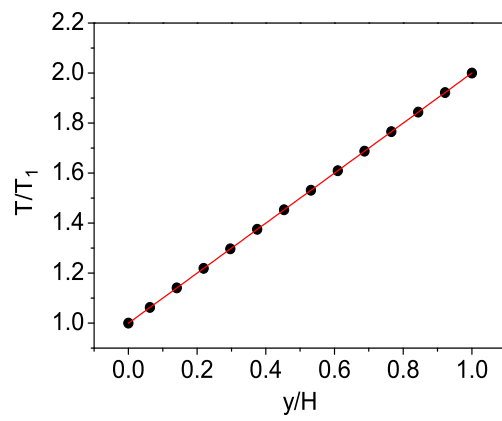
Fig. 2. Temperature profile when $C_{p1} = C_{p2}$, $\mu_1 = \mu_2$: black dot-analytic results, red line-numerical data.
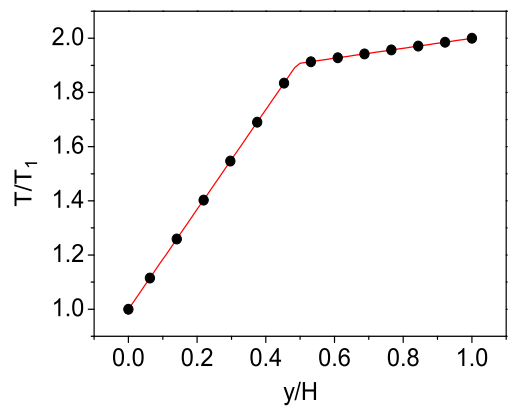
Fig. 3. Temperature profile when $C_{p2} = 3C_{p1}$, $\lambda_2 = 10\lambda_1$: black dot-FVM results, red line-the present LB prediction.
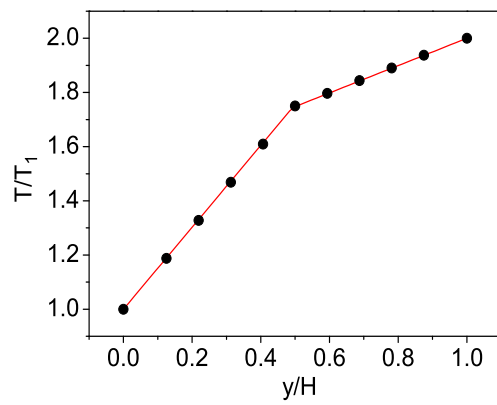
Fig. 4. Temperature profile of conjugate heat transfer between solid media: black dot-analytic results, red line-numerical data.
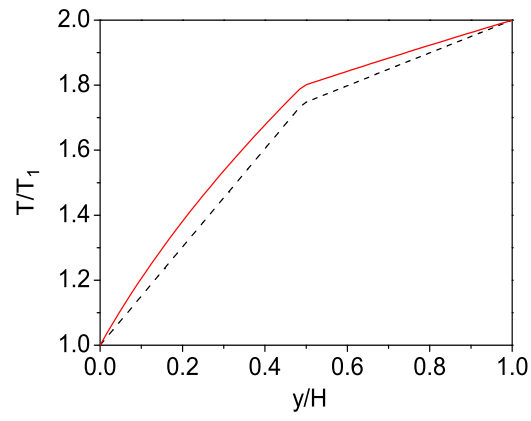
Fig. 5. Temperature profile of conjugate heat transfer between solid media: black dashed line-constant thermophysical properties, red solid line-variable thermophysical properties.
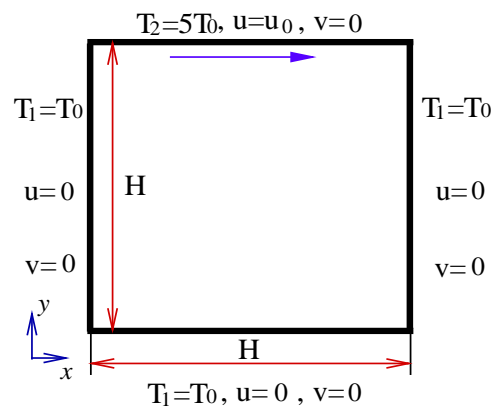
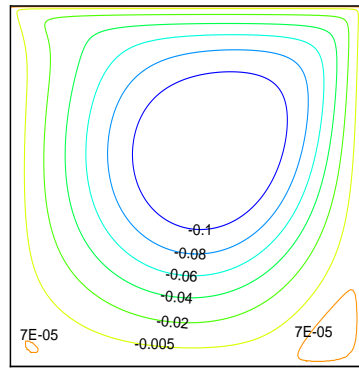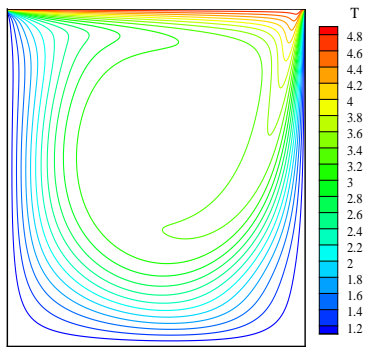Fig. 6. Schematic configuration of forced convection in lid-driven square cavity.
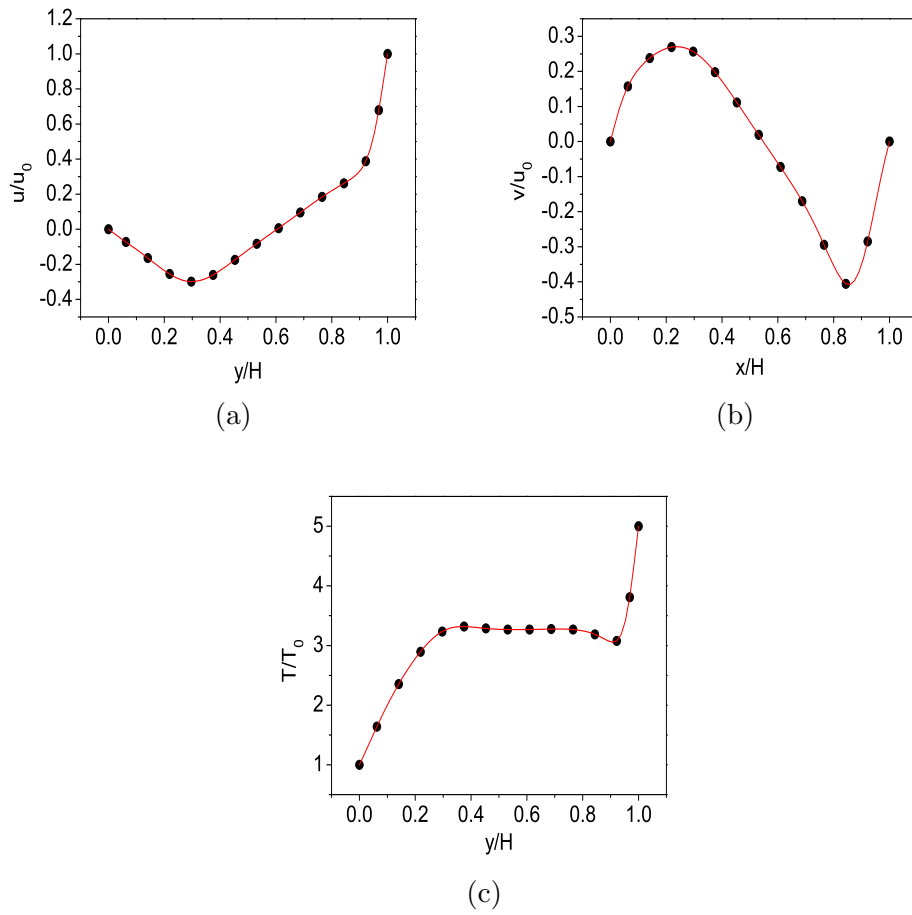
Fig. 7. Profiles of temperature and velocity along the centerlines of the cavity at $Re = 400$: red line-present LB model, black dot-vorticity streamfunction approach [26].
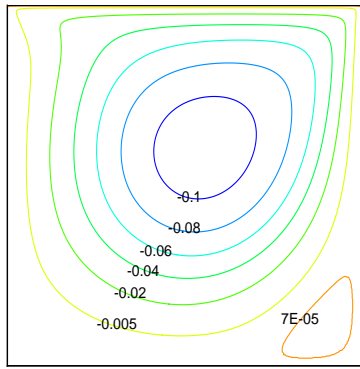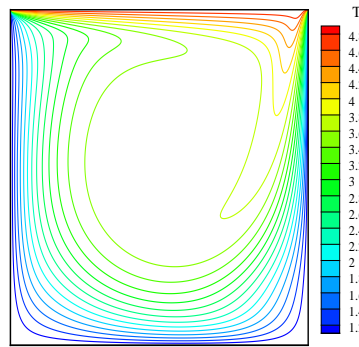
(a)　　　　　　　　　　　　　　　(b)

(c)　　　　　　　　　　　　　　　(d)

Fig. 8. Streamlines and Isotherm lines at $Re = 400$: left-constant thermophysical properties, right-variable thermophysical properties.
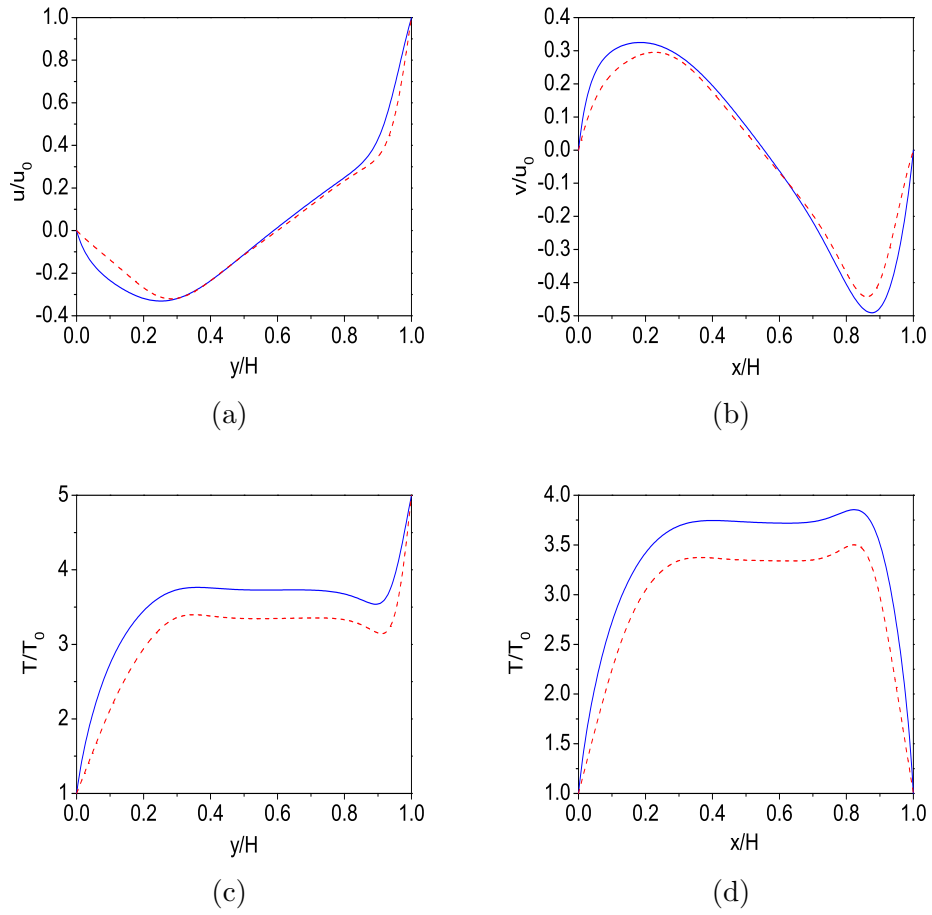
34

Fig. 9. Profiles of temperature and velocity along the centerlines of the cavity at $Re = 400$: red dasehed line-constant thermophysical properties, blue solid line-variable thermophysical properties.

Table 1

Nusselt number on walls.

	Nu_l	Nu_r	Nu_t	Nu_b
constant case	6.8424	-64.4271	42.5907	13.7958
variable case	19.4976	-37.1711	88.4859	31.1700